Development of damage state-dependent fragility functions for a MDOF structure through dynamic analyses with successive un-scaled time-histories

Jaime Abad, Thomas Ulrich, Arnaud Réveillère, Pierre Gehl

Vienna Congress on Recent Advances in
Earthquake Engineering and Structural Dynamics 2013 (VEESD 2013)
C. Adam, R. Heuer, W. Lenhardt & C. Schranz (eds)
28-30 August 2013, Vienna, Austria
Paper No. 155

Development of damage state-dependent fragility functions for a MDOF structure through dynamic analyses with successive un-scaled time-histories

J. Abad[1], T. Ulrich[1], A. Réveillère[1], P. Gehl[1]

[1] BRGM, Orleans, France

Abstract. In the context of a seismic crisis where successive aftershocks threaten to bring down previously damaged structures, damage state-dependent fragility curves may constitute a useful tool to reassess the updated vulnerability of the exposed structures. This study builds on a methodology to derive state-dependent fragility curves without record-scaling and suggests some improvements. A set of natural ground-motion records is applied multiple times to a 2D model of a reinforced-concrete moment-resisting frame building with hysteretic degradation. The relationship between the aftershock intensity measure and the engineering demand parameter (here the maximum transient drift ratio) is obtained in two steps: A modified least-squares regression is first performed between the maximum additional transient drift ratio achieved during simulation and the intensity measure, and the results are then compounded with the distribution of the initial residual drift ratio. A comparison is finally made with fragility curves derived using an incremental dynamic analysis (IDA) approach.

Keywords: Fragility curves; Dynamic analysis; Cumulative damage; Mainshock-aftershock sequences

1 INTRODUCTION

Fragility functions constitute a widespread probabilistic approach to assess the vulnerability of existing buildings to seismic hazard. Current approaches consider a single ground motion, the main shock of an earthquake, striking intact buildings or buildings that are assumed to be repaired to intact levels after previous earthquake damage.

However, as the Emilia-Romagna seismic events of May 2012 showed, a second earthquake can strike before enough time has passed to make necessary repairs. Nine days after the first earthquake of magnitude 5.9, which had caused 7 deaths and 50 injured, a second event of magnitude 5.8 hit: the building stock that had been weakened by the first shock led to more casualties, this time killing 17 and injuring over 350, for a total of 24 dead and over 400 injured. The number of homeless rose from 7000 to 20000 (Baize et al. 2012, Ioannou et al. 2012, Rossetto et al. 2012). Similarly, it is not uncommon for a strong aftershock to strike within that time window where repairs have not yet started and crisis management may be underway. It is in such a context where updated risk assessment is necessary and post-mainshock fragility functions become a powerful tool for decision-making.

This paper looks at two methods to calculate damage-state dependent fragility curves. The first of these methods (Ryu et al. 2011, Luco et al. 2011) relies on incremental dynamic analysis (IDA) (Vamvatsikos 2002), performed first on the intact structure and then on mainshock-damaged realizations. However, when the amplitude of a ground motion time-history is multiplied with a scaling factor, not all ground-motion parameters (e.g. effective duration or the effective number of cycles) scale equally (Douglas et al. 2012): in the context of cumulative damage assessment, such parameters have an impact on the hysteretic degradation, therefore potentially biasing the fragility functions.

An alternative methodology based on the work by Réveillère et al. (2012) aims to address this issue by instead performing successive dynamic analyses with natural, unscaled ground motion records. A sampling scheme makes it possible to recreate a situation where a sequence of strong seismic events occurs. The damage state information is then obtained by decomposing the maximum transient drift $\Delta_{t,max}$, which is the engineering demand parameter (EDP), into two values: the additional transient drift ($\Delta_{t,max} - \Delta_{r,t0}$) during simulation and the initial residual drift $\Delta_{r,t0}$ resulting from a previous simulation. A modified least-squares regression scheme is then performed to produce a state-dependent fragility curve out of both sets of data. Several improvements to the original approach for a better application to multiple-degree-of-freedom (MDOF) structures are described in Section 2.2.

A simple 2D four-storey reinforced-concrete structure with moment-resisting frames is tested with both methodologies. Cumulative damage from multiple earthquakes is modelled with a hysteretic degradation scheme that includes degradation of the mechanical parameters. A comparison of both methodologies is then made, including aspects relating to ground motion sampling, computational effort, as well as differences in the final fragility curves.

2 DERIVATION OF DAMAGE-STATE DEPENDENT FRAGILITY FUNCTIONS

Starting from the initial damage state (DS) of a structure after an earthquake, damage-state dependent fragility functions take the degrading effects of cumulative damage into account to estimate the probability of reaching a higher damage state, due to a following earthquake or aftershock of a given intensity happening during the time period when repairs cannot be carried out. They thus represent a useful way of considering aftershock fragility. The conditional probability for a building that has reached damage state $DS_{t0} = i$ to reach a higher damage state k when it is struck by an earthquake of intensity a, can be written, for every pair of i and k, as:

$$P\left(DS \geq k \middle| DS_{t_0} = i, IM = a\right) = \phi\left(\frac{\ln a - \ln \mu_{i,k}}{\beta_{i,k}}\right); i,k \in [0,4]; k > i \quad (1)$$

The state-dependent fragility curve is thus expressed as the normal cumulative density function ϕ of the logarithm for a given level a of the intensity measure (IM) and it can be fully characterized by the parameters $\mu_{i,k}$, the median, and $\beta_{i,k}$, the standard deviation.

The EDP chosen to quantify the damage state in this paper is the maximum transient inter-storey drift ratio, $\Delta_{t,max}$, which is assumed to make the structure reach damage state DS_k if it exceeds the threshold $\Delta_{th,k}$. Inter-storey drift ratio, referred to simply as "drift" in this paper, is the difference in horizontal displacement between the floor and ceiling of a building storey divided by the height of the storey.

2.1 Incremental dynamic analysis approach

Making use of the IDA approach to take the pre-damaged buildings into account, fragility curves are derived following two steps, which can be summarized as carrying out "back-to-back" IDA on the structure (Ryu et al. 2011, Luco et al. 2011). An IDA is first carried out on the intact structure, producing materializations of the structure in the different damage states. Subsequently, damaged materializations of the buildings are chosen and submitted each to a new IDA with the same suite of ground motions. The results of this second step are aggregated to produce the damage-state dependent fragility curves via least-squares regression between IM and EDP.

A key point in the methodology is the selection of the damaged building materializations for use in the second step IDAs. Two possibilities are presented by Ryu et al. (2011): a "deterministic" case in which the scale factor for each ground motion that causes the EDP to exactly reach the threshold for each damage state is chosen, and a so-called "uncertain" case in which a lognormal distribution around each threshold is sampled for materializations. In this study, it is proposed to use what can be referred to as a "uniform" case: the range of building materializations between two damage thresholds is sampled with a random uniform distribution, yielding fragility curves that describe the building for the whole range of a given damage state, instead of concentrating around the threshold.

2.2 Modified least-squares regression approach

This approach, based on the work by Réveillère et al. (2012), uses solely natural (unscaled) ground motions to produce damage-state dependent fragility curves, as an alternative to the IDA-based method. The core of the methodology relies on producing different materializations of the structure by storing the building state after each dynamic analysis and by subsequently subjecting these differently damaged structures to new dynamic excitations. The new materializations of the building are expected to be more vulnerable to the next ground motions than the initial structure, because of the accumulated damage during the previous earthquakes.

A procedure has been designed to obtain reliable fragility curves for each initial DS. In a first step, realizations of the intact building are submitted to the whole set of ground motions. In each simulation, two sets of drift values are tracked: The first set contains the maximum transient drift $\Delta_{t,max}$ that is reached in every storey of the structure during the dynamic analysis. This value will condition the DS reached by the structure. The other value is the initial residual drift $\Delta_{r,t0}$, i.e. the plastic drift remaining in the building at the beginning of the simulation due to nonlinear damage from a previous earthquake (for intact buildings, $\Delta_{r,t0}$ equals zero and therefore the transient additional drift equals the transient drift). The resulting damaged structures are sorted into bins depending on the DS they have attained.

Afterwards, building materializations are picked from the bin corresponding to DS1 and submitted to randomly selected ground motions. If a simulation fails to reach a higher DS, the resulting building materialization is added to the bin corresponding to the initial DS (DS1 in this case), making it available for further simulations. In case the structure does reach a higher DS, it is added to the corresponding bin, to be submitted to dynamic analysis in the following steps. Simulations are carried out until a sufficient number of materializations have been achieved for all higher damage states, Finally, the same step is repeated for the bin corresponding to the next-higher DS. In this study the number of required materializations per bin was set to 512. In practice this number is largely exceeded for the middle range of damage states.

Similarly to the "uniform" case from Section 2.1, a sampling scheme is considered to ensure that the sampled building materializations with a given DS *i* give a good overall representation of the population of that DS: every bin is divided into subpopulations based on how close the previously attained EDPs is to the drift threshold. A random process then makes sure the subpopulations are equally represented in the final result.

This 'modified' regression method owes its name to the fact that the procedure to obtain the $\mu_{i,k}$ and $\beta_{i,k}$ does not involve direct regression of the EDP on the IM. Instead, the maximum transient drift $\Delta_{t,max}$ is assumed to be composed of two parts: an initial drift $\Delta_{r,t0}$ present in the structure due to the mainshock and an additional transient drift ($\Delta_{t,max} - \Delta_{r,t0}$) added by the aftershock: it is assumed that only this second part is correlated to the the IM *a*, as given by Eq. (2) (Réveillère et al. 2012).

$$\ln\left(\Delta_{t,\max} - \Delta_{r,t_0}\right) = \ln b + c \cdot \ln a + \varepsilon \tag{2}$$

Here, *b* and *c* are linear regression parameters, whereas ε is considered a normally-distributed variable with zero mean and standard deviation β_ε. A same ground motion record is often represented several times in the cloud of data points corresponding to the damaged structures: in fact, it can be applied to different building materializations, which will generate non-identical results. Furthermore, depending on the result of the random picking process of ground motion records during the procedure, each ground motion record will be more or less represented in the data points cloud. This could lead to differences in the vulnerability functions. To filter out this effect, it was decided to give all ground motions the same weight when performing linear regression (i.e. if a ground motion record is present *n* times in the data cloud, every corresponding result will have a weight of *1/n*).

For a building with a given initial residual drift $\Delta_{r,t0} = \Delta_0$, the probability that maximum transient drift surpasses the drift threshold $\Delta_{th,k}$ for damage state DS_k can thus be defined as the probability that $(\Delta_{t,max} - \Delta_{r,t0})$ equals $(\Delta_{th,k} - \Delta_0)$ (Réveillère et al. 2012):

$$P\left(DS \geq k \middle| \Delta_{r,t0} = \Delta_0, IM = a\right) = \phi\left[\frac{\ln\left(b \cdot a^c\right) - \ln\left(\Delta_{th,k} - \Delta_0\right)}{\beta_\varepsilon}\right] \tag{3}$$

The next step is to interpret the initial residual drift $\Delta_{r,t0}$ by studying the distribution of residual drifts within each damage state: $f(\Delta_{r,t0} | DS_{t0} = i)$. By performing numerical integration over Δ_0 between 0 and $\Delta_{th,i+1}$ (the residual drift cannot exceed the drift threshold), the connection between EDP and IM is established in Eq. (4) (Réveillère et al. 2012). Multiple assumptions over $f(\Delta_{r,t0} | DS_{t0} = i)$ are possible, but in this paper it was chosen to directly integrate over the values obtained through dynamic analysis (i.e. discrete summation instead of integration over a continuous idealization of the initial drift repartition by a Gaussian, as done by Réveillère et al. 2012).

$$P\left(DS \geq k \middle| DS_{t_0} = i, IM = a\right) = \int_0^{\Delta_{th,i+1}} P\left(DS \geq k \middle| \Delta_{r,t0} = \Delta_0, IM = a\right) \cdot f\left(\Delta_{r,t0} \middle| DS_{t0} = i\right) d\Delta_0 \tag{4}$$

Finally, a lognormal cumulative distribution is fitted to the resulting curve to obtain the defining parameters $\mu_{i,k}$ and $\beta_{i,k}$ for smooth damage-state dependent fragility functions.

3 APPLICATION TO A FOUR-STOREY STRUCTURE

3.1 Structural model

The chosen structure consists of a reinforced concrete moment-resisting bare frame, as described in Abo El Ezz (2008) and Romao (2002). The building is comprised of four storeys of 3 m height and three bays of 5 m length. All columns share the same square 0.45 x 0.45 m section and steel reinforcement (4∅16+4∅12 = 1822.12 mm²) and all beams have a rectangular section of 0.6 m height by 0.3 m width but with five different configurations of steel reinforcement at member ends, labelled A through E in Figure 1 and described in Table 1.

Modelling was carried out using a lumped plasticity approach, which localizes the nonlinear behaviour in zero-length rotational spring elements at the ends of the member, modelling the rest of the member as linear-elastic. Mechanical cyclic behaviour of the springs follows the modified Ibarra-Krawinkler deterioration model (Ibarra et al. 2005, Lignos and Krawinkler 2009), which allows taking hysteretic strength and stiffness degradation of the springs into account, as well as second order effects. The

parallel version of OpenSees software (version 2.4.0.10, McKenna et al. 2000) was used, where the Ibarra-Krawinkler formulation is implemented for a bilinear hysteretic scheme (Altoontash 2004).

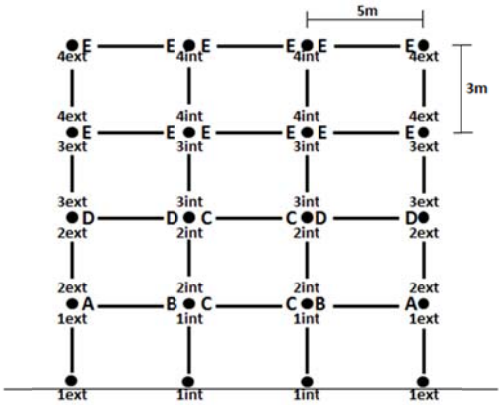

Figure 1. Frame geometry (Abo El Ezz, 2008)

Table 1: Beam section reinforcement area and yield moments

Beam sections	Upper long. steel layer	$A_{s,sup}$ mm²	$M_{y,sup}$ kNm	Lower long. steel layer	$A_{s,inf}$ mm²	$M_{y,inf}$ kNm
Section A	3∅16+2∅12	829.38	219	3∅12+2∅10	496.37	134
Section B	2∅10+2∅16	559.20	160	3∅10+2∅10	496.37	130
Section C	2∅16+2∅12	628.32	173	4∅10	314.16	87
Section D	2∅16+2∅12	628.32	173	3∅12+2∅10	496.37	134
Section E	3∅12+2∅10	496.37	127	4∅10	314.16	91

A series of parameters, listed in Table 2, were determined to define the backbone curve and degradation coefficients for the Ibarra-Krawinkler formulation. Values for the initial elastic rotation stiffness K_e and the yield moment M_y in both directions were listed in Abo El Ezz (2008), with one value of K_e applying to all columns, and another to all beams. Different yield moments are defined for the columns depending on axial load (Figure 1, Table 3). Parameters beyond the yield point, including the strain hardening ratio a_s, the plastic rotation capacity θ_p, post-capping deformation capacity θ_{pc}, residual strength and ultimate rotation θ_u, were estimated by calibration with an available global capacity curve where possible, otherwise following the recommendations in Haselton et al. (2007). Moderate values of the degradation coefficient Λ were chosen for the three modes of hysteretic degradation: 0.15 for the basic strength degradation (Λ_S) and 0.05 for unloading stiffness deterioration (Λ_K).

Table 2: Ibarra-Krawinkler spring parameters

	K_e kNm	Λ_S	Λ_K	θ_p rad	θ_{pc} rad	θ_u rad	a_s
Beam section	314600	0.15	0.05	0.013	0.20	0.215	0.01
Column section	331650	0.15	0.05	0.013	0.20	0.215	0.01

Table 3: Column section yield moments M_y for external and internal columns in each floor

Floor	1	2	3	4
External columns	144 kNm	168 kNm	189 kNm	210 kNm
Internal columns	161 kNm	205 kNm	247 kNm	247 kNm

The elastic members to which the joints connect are modelled using a Young's modulus of 29 GPa for concrete, as given by Romao (2002), and the full moment of inertia. Furthermore, in order to properly model the interaction between the member and its plastic hinges, values of elastic rotation stiffness and member Young's modulus were adjusted following the recommendations by Ibarra & Krawinkler (2005).

3.2 Proposed damage states for damage state-dependent fragility curves

The Ghorabah (2004) damage scale for ductile moment-resisting frames, based on the inter-storey drift ratio, was employed:

Table 4. Drift thresholds used for the studied structure (Ghobarah 2004)

Damage level:	Light	Moderate	Irreparable	Severe	Collapse
Drift threshold:	0.2%	0.4%	1.0%	1.8%	3.0%

These values are assumed to remain constant regardless of the previous state of the structure. In order to avoid convergence and numerical instability problems, the "collapse" damage state is not taken into account in this study, instead merging that "severe" and "collapse" damage states into a single 'near collapse/collapse' damage state.

3.3 Ground-motion selection

3.3.1 Scalable ground motions for incremental dynamic analysis approach

A dataset of 15 ground motions proposed by Iervolino et al. (2012) in the frame of FP7 project REAKT and containing records from the European Strong-Motion Database (Ambraseys et al. 2004), was explicitly conceived for application in incremental dynamic analysis. This was ensured by choosing records that fit within the expected values of ground motion prediction equations (GMPEs) for intensity measures relevant to IDA, such as peak ground acceleration, peak ground velocity, Arias intensity, significant duration, Housner intensity and spectral pseudo-acceleration. Scaling is performed with respect to the spectral pseudo-acceleration at the fundamental period of the structure $SA(T_1)$ where T_1=0.615 s.

3.3.2 Unscaled ground motions for modified least-squares regression approach

A large set of strong-motion records is required to build robust fragility functions. A dataset of 221 accelerograms has been assembled, using records from the European Strong-Motion Database (Ambraseys et al. 2004) and from the PEER NGA database (Chiou et al. 2008). Attention was paid to assembling a dataset in which stronger ground motions are well represented to ensure that the right part of the fragility functions, which is the most interesting since it corresponds to higher damage states, will be adequately constrained, and that the log-normal curve is not fit solely by the points near the origin, which correspond to the weaker ground motions. Consequently, a subset of records has been selected in order to achieve a better overall distribution of PGA. To do that, the interval of acceleration [0,10] m/s² has been uniformly divided in 20 bins. Then, records have been picked from the main dataset and sorted into the bins. When the number of records for a bin exceeds a given limit (set between 10 and 18, depending on the PGA), the bin is closed, and the remaining records with the same characteristics are discarded.

4 RESULTS AND DISCUSSION

The necessary dynamic analyses were run to generate the fragility functions following both methods. The results are summarized in Table 5. Figure 2 presents the curves obtained using the "back-to-back"

IDA approach (B2B-IDA) and Figure 3 those corresponding to the "modified regression" approach (MR). In both figures, the colour of the line represents the initial damage state, while the line style represents the final damage state. It is noted that, despite the much smaller selection of ground motions, the calculation effort for the back-to-back IDA approach is much higher: 28000 simulations for the MR approach vs. 116000 simulations required for B2B-IDA. Although it is possible to reduce the number of IDA simulations using optimization algorithms, such as "hunt and fill" procedures (Vamvatsikos 2002), it should be noted that the number of simulations required for B2B-IDA is proportional to the square of the number of accelerograms, and that only 15 records were used in this article.

Table 5: Median $\mu_{i,k}$ and standard deviation $\beta_{i,k}$ values characterizing the state-dependent fragility curves for all combinations of initial (DS_i) and final (DS_k) damage state for both approaches.

Damage states		"Modified regression"		"Back-to-back" IDA	
DS_i	DS_k	$\mu_{i,k}$	$\beta_{i,k}$	$\mu_{i,k}$	$\beta_{i,k}$
		m/s²	-	m/s²	-
0	1	1.03	0.41	1.11	0.11
0	2	2.25	0.41	3.06	0.17
0	3	6.33	0.41	8.02	0.30
0	4	12.30	0.41	11.41	0.36
1	2	1.98	0.42	2.97	0.16
1	3	5.78	0.41	8.15	0.31
1	4	11.29	0.41	11.35	0.36
2	3	4.83	0.45	6.87	0.41
2	4	9.82	0.44	9.69	0.38
3	4	6.47	0.86	6.27	0.55

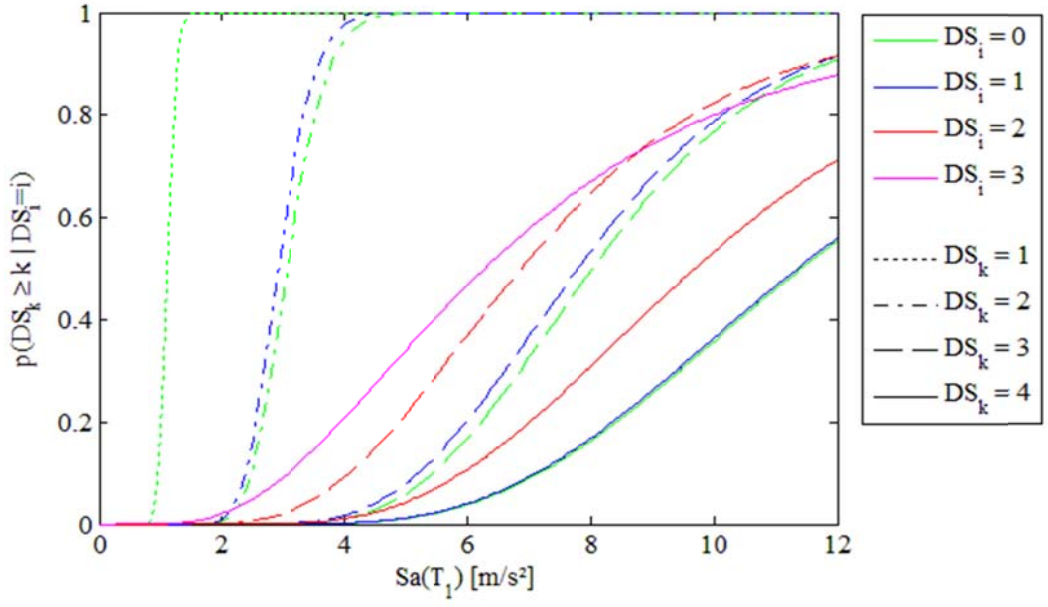

Figure 2. Damage-state dependent fragility curves using "back-to-back" IDA approach. Initial DS represented by colour, final DS represented by line style.

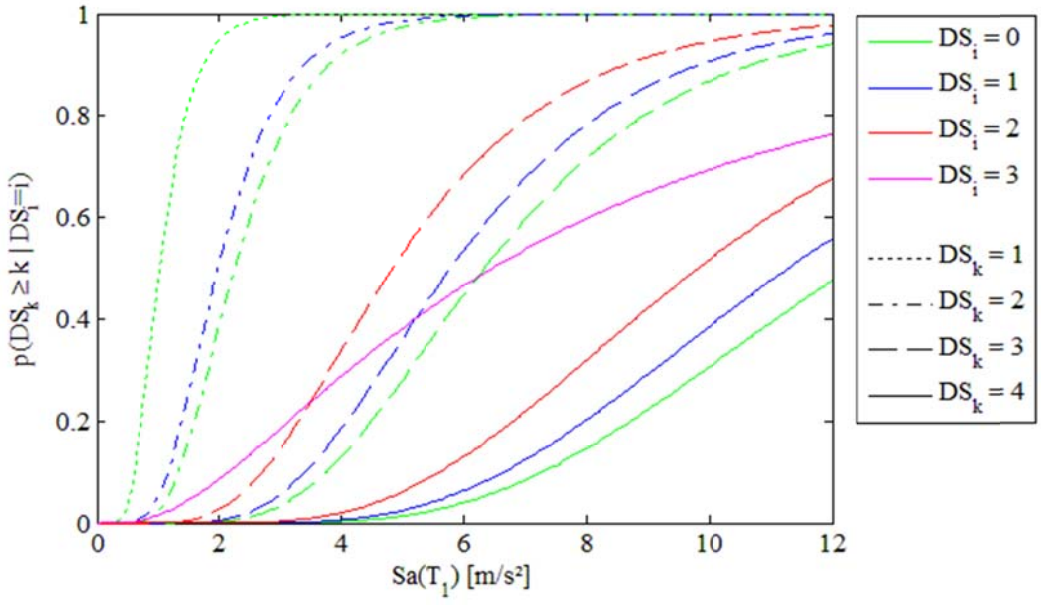

Figure 3. Damage-state dependent fragility curves using modified least-squares regression approach. Initial DS represented by colour, final DS represented by line style.

As can be observed, the B2B-IDA curves are steeper due to lower standard deviation values and, for $DS_k < 4$, they are shifted towards the right due to higher medians. The low standard deviation can point towards a low variability in the sample. This could be due to intrinsic differences in the two approaches, it could suggest that the chosen suite of 15 accelerograms may be too small, or it could indicate that the role of mechanical degradation is being understated: in the B2B-IDA method, exclusively one mainshock and one aftershock are taken into account, so all degradation is due to these two events. In reality, smaller aftershocks that may also induce some material degradation are not uncommon, affecting buildings in higher damage states especially: the MR approach allows taking their effect into account.

The shift towards the left in the MR curves for lower DS_k is also a signifier of mechanical degradation affecting behaviour more prominently: weaker (i.e. lower IM) aftershocks become more likely to send the softened structure into higher damage states in this approach. It is noted that this shift to the right disappears for $DS_k = 4$ (solid lines): B2B-IDA curves are here slightly to the right of MR curves, meaning both approaches predict similar medians for collapse.

However, this rightward shift is present even for $DS_i = 0$ (green curves), which precludes it being a consequence of the influence of cumulative damage exclusively. Focusing on this initial damage level, the intrinsic differences between both approaches become apparent. For high levels of damage especially, the ground motions used in both approaches differ heavily: the high level of scaling imposed on the B2B-IDA ground motions necessarily alters their frequency content. Fragility curves obtained with a set of natural accelerograms where a value such as the PGA covers wide range are going to differ from those obtained with a set of accelerograms where PGA is always high due to amplitude scaling. Furthermore, IDA curves are often non-monotonous and can cross the same threshold at multiple scaling levels whereas in this study the lowest scaling level to reach a higher damage state was always retained, biasing results towards the left.

The imposition of the uniform sampling system in the MR approach also appears to have an influence on this shift to the right in the MR results: when materializations of the structure closer to the lower damage threshold are better represented in the total population, there is an increased influence of higher intensity ground motions on the median.

It should likewise be noted that, instead of focusing on an underestimation of mechanical degradation in the B2B-IDA approach, the opposite interpretation is also possible, whereby high variability in the MR sample could mean that the approach overestimates the effect of mechanical degradation. This could be caused by allowing the generated mainshock-aftershock sequences to feature too many earthquakes that increase fragility without altering the damage state, suggesting that it might be necessary to limit the total amount of events that can be applied during one loading history, possibly to better match the repartition of aftershocks in real seismic crises. High variability may also be explained by the procedure to fit a cumulative log-normal distribution to the numerically integrated curve. One last possible explanation would be that the MR method may not be taking the relationship between mechanical degradation and damage state sufficiently into account, which would imply that the chosen couple of residual drift and additional transient drift may not be able to describe the initial and final damage states of the structure well enough: surpassing a certain transient drift threshold may not be enough to quantify damage for a building with significant mechanical degradation.

5 CONCLUSIONS

A methodology to calculate damage state-dependent fragility curves using only natural accelerograms is presented and compared to an IDA-based approach via application to a test structure. The proposed approach requires more ground motion records to generate results, but far less computational effort, and avoids potential biases induced by amplitude-scaling.

Higher variability and higher vulnerability in the lower damage states, represented by higher standard deviation and lower medians, in the proposed method is explained by the higher influence played by cumulative damage as well as intrinsic differences between the two approaches. Probability of collapse, however, is roughly the same for both methods.

In particular, the role played by aftershocks that may not cause the structure to enter a higher damage state (i.e. the ones may not cause its maximum transient drift to surpass the next higher threshold) but do cause cumulative damage in the form of structural degradation, requires closer attention. The "back-to-back" IDA approach doesn't take this type of aftershock into account, which might result in underestimation of their influence, but it is difficult to say whether they are properly taken into account or even overestimated in the proposed "modified regression" method. Improvements in the generation of mainshock-aftershock chains may be necessary, such as limiting the number of total aftershocks to a certain value.

The influence of cumulative damage also raises questions about the ability of currently used inter-storey drift ratio thresholds to properly represent damage in the context of time-dependent vulnerability, where the degradation of mechanical parameters over the course of multiple ground-motions may play a key role in altering the displacement capacities of the structure.

ACKNOWLEDGEMENTS

The research featured in this paper has been carried out within the framework of the REAKT Project, funded by the European Commission's Seventh Framework Program [FP7/2007-2013] under grant agreement n° 282862.

REFERENCES

Abo El Ezz, A. (2008). Deformation and strength based assessment of seismic failure mechanisms for existing RC frame buildings. Master's dissertation, ROSE School, Italy.

Altoontash, A. (2004). Simulation and damage models for performance assessment of reinforced concrete beam-column joints. PhD dissertation, Stanford University, California.

Ambraseys, N., Smit, P., Douglas, J., Margaris, B., Sigbjornssaor, R., Olafsson ,S., Sugadolc, P.and Costa, G. (2004). Internet site for European strong-motion data, *Bolletino de Geofisica Teorica ed Applicata*, **45**: 113-129

Baize, S., Vanoudheusden, E., Guéguen, P., Martin, P.-O., Perrotin, P., Chever, L., Cuyeu, P. and Verdoux, M. (2012). La séquence sismique de Mai 2012 en Emilie-Romagne (région de Ferrara à Modena). AFPS field report. Association Française du Génie Parasismique, Paris, France.

Chiou, B., Darragh, R., Gregor, N. and Silva, W. (2008). NGA Project Strong-Motion Database. *Earthquake Spectra* **24:** 23-44

Douglas, J., Gehl, P., Réveillère, A. and Karapetrou, S. (2012). Strong-motion descriptors. Deliverable D5.2. FP7 project REAKT: Strategies and tools for Real Time Earthquake Risk Reduction.

Ghobarah A. (2004). On drift limits with different damage levels. In: *Proceedings of International Workshop on Performance-based seismic design concepts and implementation*; June 28th – July 1st, 2004, Bled, Slovenia.

Haselton, C.B., Liel, A.B., Lange, S.T. and Deierlein, G.D. (2008). Beam-Column Element Model Calibrated for Predicting Flexural Response Leading to Global Collapse of RC Frame Buildings. PEER Report 2007/03. Pacific Earthquake Engineering Research Center, College of Engineering, University of California, Berkeley.

Ibarra, L.F. and Krawinkler, H. (2005). Global Collapse of Frame Structures under Seismic Excitations. Report No. 152. Final Report on PEER Project 3192002: Engineering Assessment Methodology.

Ibarra, L.F., Medina, R.A. and Krawinkler, H. (2005). Hysteretic models that incorporate strength and stiffness degradation. *Earthquake Engineering and Structural Dynamics* **34**: 1489-1511.

Iervolino, I., Baltzopoulos, G. and Chioccarelli E. (2012). Record Selection Exercise Report (draft). FP7 project REAKT: Strategies and tools for Real Time Earthquake Risk Reduction.

Ioannou I., Borg, R., Novelli, V., Melo, J., Alexander, D., Kongar, I., Verrucci, E., Cahill, B. and Rossetto, T. (2012). The 29th May Emilia Romagna Earthquake. EPICentre Field Observation Report No. EPI-FO-290512. UCL EPICentre, University College London, London, United Kingdom.

Lignos, D.G. and Krawinkler, H. (2009). Sidesway collapse of deteriorating structural systems under seismic excitations, Rep.No.TB 172, The John A. Blume Earthquake Engineering Research Center, Stanford University, Stanford, CA.

Lignos, D.G. and Krawinkler, H. (2012). Development and Utilization of Structural Component Databases for Performance-Based Earthquake Engineering. *Journal of Structural Engineering*, doi: 10.1061/(ASCE)ST.1943-541X.0000646.

Luco, N., Gerstenberger, M.C., Uma, S.R., Ryu, H., Liel, A.B. and Raghunandan, M. (2011). A methodology for post-mainshock probabilistic assessment of building collapse risk. In: *Proceedings of the Ninth Pacific Conference of Earthquake Engineering (PCEE 2011)*; April 14-16, 2011, Auckland, New Zealand.

McKenna, F., Fenves, G. L., Scott, M. H., and Jeremic, B. (2000). Open System for Earthquake Engineering Simulation (OpenSees). Pacific Earthquake Engineering Research Center, University of California, Berkeley, CA.

Réveillère, A., Gehl, P., Seyedi, D., and Modaressi, H. (2012). Development of seismic fragility curves for mainshock-damaged reinforced concrete structures. In: *Proc. 15th World Conference of Earthquake Engineering (WCEE)*; September 24-28, 2012, Lisbon, Portugal.

Romao, X. (2002). Novos modelos de dimensionamiento sismico de estruturas. Master's dissertation, Universidade do Porto, Portugal.

Rossetto, T., Alexander, D., Verrucci, E., Ioannou, I., Borg, R., Melo, J., Cahill, B., Kongar, I. (2012). The 20th May Emilia Romagna Earthquake. EPICentre Field Observation Report No. EPI-FO-200512. UCL EPICentre, University College London, London, United Kingdom.

Ryu, H., Luco, N., Uma, S.R. and Liel, A.B. (2011). Developing fragilities for mainshock-damaged structures through incremental dynamic analysis. In: *Proceedings of the Ninth Pacific Conference of Earthquake Engineering (PCEE 2011)*; April 14-16, 2011, Auckland, New Zealand.

Vamvatsikos D. (2002). Seismic Performance, Capacity and Reliability of Structures as seen through Incremental Dynamic Analysis. Ph.D Dissertation, Report No. RMS-46 and Report No. TR-151, Stanford University, Stanford.